Chemical Characterization of Atmospheric Dust with Spectroscopic Lidar

Avinash Yadav[(a)], Boyan Tatarov[(a)], Rui Song[(b)], Adrian Ghita[(c)], Detlef Müller [(a)]
[(a)] *Department of Physics, Astronomy and Mathematics, University of Hertfordshire, College Lane, Hatfield, AL10 9AB, Hertfordshire, United Kingdom*
[(b)] *National Centre of Earth Observation, Atmospheric, Oceanic and Planetary Physics, University of Oxford, Oxford, OX1 3PU, Oxfordshire, United Kingdom*
[(c)] *School of Life and Medical Sciences, University of Hertfordshire, College Lane, Hatfield, AL10 9AB, Hertfordshire, United Kingdom*
Lead Author e-mail address: a.yadav@herts.ac.uk

Abstract: We present spectral signatures of a distinct dust layer advected to the UK from Northwest Africa on 01 – 02 May 2024 (Aerosol Optical Depth (AOD) = 0.19, mean Lidar Ratio (LR) = 51 ± 11 sr, Particle Linear Depolarization Ratio (PLDR) = 0.28 ± 0.01) with a 532 nm laser excitation. The spectral analysis identified a characteristic Raman-shifted peak at 571.0 nm ± 1.3 nm (corresponding to 1284 ± 40 cm^{-1} Raman shift) alongside enhanced backscatter intensity within the 542.9 – 554.4 nm wavelength range (377 – 759 cm^{-1}). These spectral signatures were consistently detected within the dust plume boundaries while remaining undetectable outside of it, establishing their direct link to the dust intrusion. Laboratory-acquired Raman spectra of collected dust particles corroborated the lidar measurements.

1. Introduction

Characterizing the chemical composition of the atmosphere is essential for understanding critical atmospheric processes, including radiative forcing, cloud microphysics, and heterogeneous chemistry, as well as for evaluating their impacts on climate and environment [1]. Conventional in-situ techniques provide accurate measurements of chemical composition in controlled laboratory environment but are limited in spatial coverage and often require direct access to the sampling region [2]. Active remote-sensing techniques, particularly lidars, offer a powerful alternative by enabling continuous, range-resolved observations, though they are typically limited to optical properties [3].

Spectroscopic lidar extends traditional lidar capabilities by providing more comprehensive, range-resolved chemical fingerprints of atmospheric constituents based on their distinctive molecular signatures. In this study, we present a spectroscopic lidar approach designed to identify and characterize the chemical fingerprint of the atmosphere with enhanced spectral coverage and sensitivity. We describe the system concept, measurement strategy, and initial results that demonstrate its potential for atmospheric monitoring and environmental assessment.

2. Methodology/Instrumentation

A novel spectroscopic lidar infrastructure (LITES: Lidar Innovations for Technologies and Environmental Sciences) specifically designed to bridge the laboratory compositional characterization and lidar profiling has been developed at the University of Hertfordshire, UK.

This system represents a systematic attempt to measure 32-channel Raman and fluorescence spectra from atmospheric constituents with range-resolved vertical profiling. Each channel corresponds to distinct wavelengths capturing Raman-shifted returns, which allow detailed spectral characterization of backscattered atmospheric signals. The multi-channel configuration enables concurrent measurement of diverse aerosol constituents, their scattering characteristics, and spectral signatures. Laboratory measurements using Raman micro-spectroscopy is an integrated part of this facility, which provides reference data for validation of lidar observations. More comprehensive details of instrumentation and methodology are documented in [4 – 5]. This work examines spectrally resolved

atmospheric backscatter signals during a Saharan dust transport to the UK on 01 – 02 May 2024. The 32-channels of the signal detection unit covered a spectral range of approximately 40 nm between 542.9 nm – 582.5 nm, with approximately 1.27 nm spectral resolution per channel. This wavelength window was selected to detect mineral dust constituents including oxides, silicates, and carbonates, which display characteristic Raman features within this lower wavenumber region, observed during laboratory measurements.

3. Results

Range-corrected backscatter measurements (Figure 1) identified an elevated dust plume spanning 2 – 5 km altitude above ground level (agl). Upper-tropospheric clouds appeared between 6 – 12 km. During 21:00 – 23:00 UTC, boundary layer clouds appeared within the dust layer at 3 – 4 km.

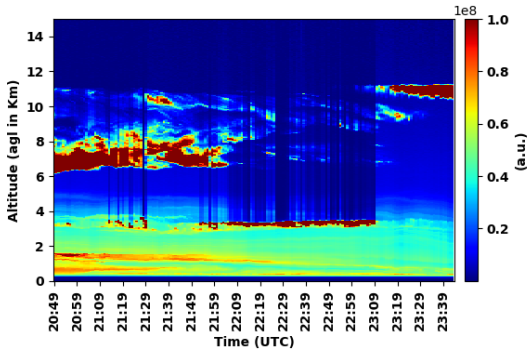

Figure 1. Spatiotemporal variation of range-corrected signals at 532 nm.

Vertical distributions of aerosol optical parameters at 532 nm for the period 23:15 to 23:44 UTC on 01 May 2024 over Hatfield, United Kingdom (51.75° N, 0.24° W, 88.5 m asl) are shown in Figure 2.

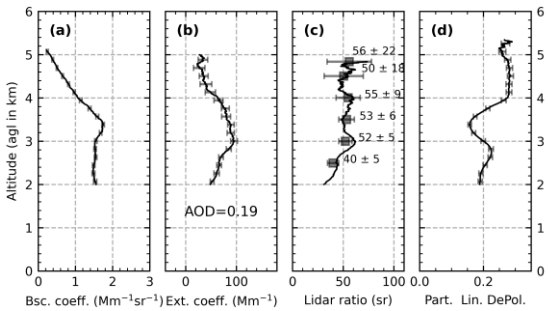

Figure 2. Dust optical properties between 23:15 to 23:44 UTC on 01 May 2024: (a) Back scatter coefficients ($Mm^{-1}sr^{-1}$), (b) Extinction coefficients (Mm^{-1}), (c) Lidar ratio (sr) and (d) Particle linear depolarization ratio.

The lidar derived optical properties, i.e., aerosol optical depth (AOD = 0.19), lidar ratio (mean LR = 51 ± 11 sr), and particle linear depolarization ratio (PLDR = 0.28 ± 0.01), complemented with Aerosol Robotic Network (AERONET) observations, Copernicus Atmosphere Monitoring Services (CAMS) reanalysis observations, and trajectory analysis confirmed the presence of Saharan dust [5].

Figure 3 displays the spectrally resolved and vertically resolved Raman signals averaged between 23:15 – 23:59 UTC.

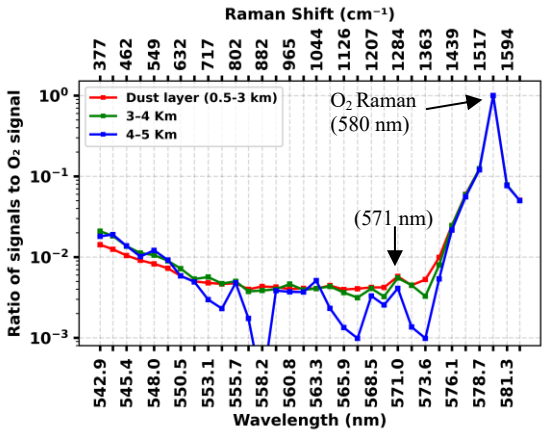

Figure 3. Spectral– and range–resolved signals between 23:15 – 23:59 UTC.

Raman spectra were extracted for three altitude intervals: the complete dust column (0.5 – 3 km), additional separate spectra between 3 – 4 km and 4 – 5 km. Normalization was performed relative to the O_2 Raman line (580 ± 1.3 nm). A pronounced spectral feature emerged at 571.0 ± 1.3 nm (equivalent to 1284 ± 40 cm^{-1} Raman shift) throughout the dust column. Laboratory Raman analysis of a Saharan desert dust sample revealed a similar feature at 1350 cm^{-1} (Figure 4).

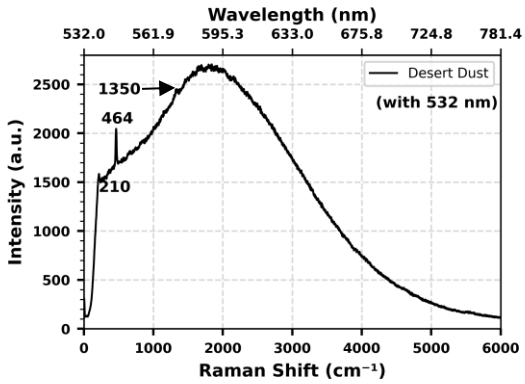

Figure 4. Raman spectra of Saharan desert dust measured with 532 nm excitation.

However, direct quantitative comparison of the laboratory and lidar Raman features remains limited due to different spectral resolutions as laboratory measurements achieve 0.05 nm (1 – 2 cm^{-1}) versus lidar's 1.3 nm (40 cm^{-1} at 532 nm excitation) and the absence of the independent knowledge of the compositional constituents of the transported dust.

Beyond 4 km altitude, this signature weakens, consistent with diminished Raman returns and decreased particle loading (Figure 1). Notably, the 571.0 nm feature exhibits approximately 1/100th the intensity of the O_2 Raman signals at 580.0 ± 1.3 nm, both acquired simultaneously under identical atmospheric conditions. This intensity ratio reflects the low dust concentration relative to molecular oxygen, yet the feature's reproducibility across the dust layer establishes its significance as a fingerprint.

Complementing the 571.0 nm peak, elevated returns appeared in channels spanning 542.9 nm to 554.4 nm (377 cm^{-1} to 759 cm^{-1} Raman shift). This spectral window captures vibrational modes diagnostic of mineral constituents: quartz (464 cm^{-1}), corundum (417 cm^{-1}), feldspars (510 cm^{-1}), clay phases including kaolinite (635 cm^{-1}), and iron oxides such as hematite (290 cm^{-1}), measured in LITES laboratory with the Raman microscopy [6]. The absence of fine resolved signatures reflects limited lidar spectral resolution. The smooth logarithmic decrease between 542.9 and 554.4 nm in the dust spectrum may indicate fluorescence contributions from certain minerals. Reichardt et al. [7] documented fluorescence from Saharan dust over Germany, observing maximum emission at 455 nm with gradual decline toward 680 nm. Though employing 355 nm excitation, their spectral gradient resembles our observations. Current data cannot definitively attribute the contributions from Raman scattering, fluorescence, or their superposition in the spectra shown in Figure 3.

Figure 5 compares the Raman spectra from low-altitude cloud (3 – 4 km) against the underlying dust layer (0.5 – 3 km) during 22:00 – 23:00 UTC, revealing altitude-dependent spectral differentiation. The 571.0 ± 1.3 nm (1284 ± 40 cm^{-1}) signature persistent in Figure 3 remains evident within the dust mass. Conversely, the Raman spectrum of cloud (3 – 4 km) lacks this feature, confirming its exclusive association with mineral aerosols rather than liquid droplets. This absence of the spectrum in the cloud layer reinforces its attribution to the dust plume identified in time-averaged retrievals. Similarly, enhanced backscattered signals in shorter-wavelength range (542.9 – 554.4 nm) characterize the dust layer (Figure 3 and Figure 5) while remaining undetectable in the cloud spectrum.

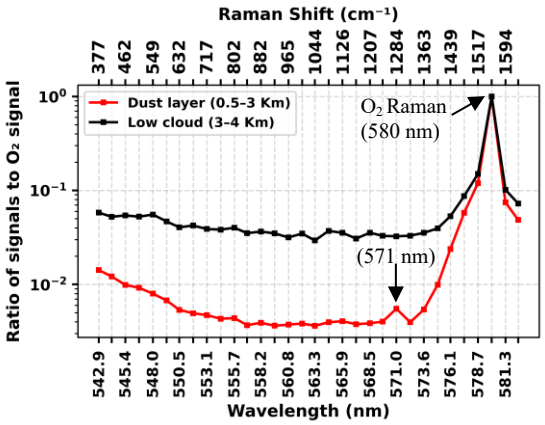

Figure 5. Spectral comparison of the dust layer and clouds between 22:00 to 23:00 UTC.

The absence of both the 571.0 nm peak and shorter-wavelength enhancements within the cloud returns confirms mineral-specific origins and demonstrates spectroscopic lidar's capacity for aerosol-type discrimination via dust-specific intrinsic vibrational modes. This capability enables dust-cloud separation in mixed-phase atmospheric scenarios. Elevated cloud spectrum intensity likely originates from fluorescence or multiple scattering within droplets, contributing to overall spectral characteristics.

To quantify this spectral distinction, linear regression was applied to the logarithmic ratios

of wavelength-dependent signals (542.9 – 554.4 nm) normalized to the oxygen Raman line across 0.5 – 1 km, 1 – 2 km, 2 – 3 km, the integrated dust column (0.5 – 3 km), and lower cloud (3 – 4 km). Derived slopes consistently approximate -0.08 per nm throughout dust altitudes versus -0.03 per nm for cloud, substantiating mineral attribution of shorter-wavelength enhancements. Feature reliability is supported by photon-count relative uncertainties below 10% for all the spectra below 4 km altitude, which validates both the 571.0 nm signature and initial-channel intensity enhancements.

4. Conclusion

The methodological approach of a spectroscopy lidar presented in this contribution demonstrates an advancement over solely measuring optical parameters (backscatter, extinction, and depolarization ratios) as it offers a more accurate identification of dust aerosols. Our observations of a reproducible Raman peak at 571.0 ± 1.3 nm (1284 ± 40 cm^{-1}) alongside amplified returns spanning 542.9 – 554.4 nm demonstrate that mineral-specific vibrational modes remain detectable in a weak atmospheric dust loading (AOD = 0.19).

Critically, these spectral signatures disappeared from cloud and outside of the dust layer, establishing spectroscopic lidar's capacity to resolve compositional boundaries that elude traditional optical-only retrievals. The enhanced shorter-wavelength response corresponds precisely to the vibrational fingerprint region of primary desert minerals—silicates, phyllosilicates, feldspars, and iron oxides—validated through controlled laboratory Raman microscopy. This spectral-spatial correlation confirms that range-resolved Raman spectroscopy can bridge the compositional gap between remote sensing and in-situ measurements.

Our findings reveal that successful mineral identification persists despite some fundamental constraints: inherently weak inelastic scattering cross-sections, moderate spectral resolution (1.3 nm/40 cm^{-1}), and weak dust loading that suppresses particulate number density by orders of magnitude compared to laboratory samples. The consistency of spectral slopes across independent altitude bins (−0.08 nm^{-1} for dust versus −0.03 nm^{-1} for cloud) provides quantitative metrics for automated aerosol classification algorithms.

These results demonstrate a transformative pathway: under the challenges to observe discrete and fine mineral signatures, robust and persistent spectral signatures can be exploited for gaining information on the chemical composition of mineral dust.

This study confirms that atmospheric Raman spectroscopy has capability to transition high-resolution laboratory measurements into real-time remote observations, positioning spectroscopic lidar as an essential tool for next-generation aerosol characterization.

5. References

[1] Raes, F. et al., “Formation and cycling of aerosols in the global troposphere,” Atm. Env., 4215-4240 (2000).

[2] Kandler, K. et al., “Electron microscopy of particles collected at Praia, Cape Verde, during the Saharan Mineral Dust Experiment: particle chemistry, shape, mixing state and complex refractive index”, *Tellus B: Chemical and Physical Meteorology*, 63(4), 475-496 (2011).

[3] Ansmann, A. and Müller, D., “Lidar and Atmospheric Aerosol Particles”. In Lidar (Weitkamp, C., 2005), Chap. 4.

[4] Tatarov, B. and Müller, D., “LITES: rotational Raman spectra of air molecules measured by high-resolution-spectroscopy lidar,” Opt. Lett. 46, 5173-5176 (2021).

[5] Yadav, A. et al., “Characterizing the Saharan dust transported to the UK through lidar ratio, particle depolarization, and spectroscopic measurements,” Atm. Env., 121613, 363 (2025).

[6] Yadav, A. et al., “Investigation of Raman spectra of mineral dust for identifying the chemical composition of desert dust by Raman lidar”, in Dust 2025 Conf., 81 (2025).

[7] Reichardt, J. et al., “Fluorescence spectra of atmospheric aerosols”, Atmos. Chem. Phys., 25, 5857-5892 (2025).